# Applying Neural Networks to Identify possible sources for Ultra-relativistic Electrons found in Nonthermal Filaments: Project Proposal

Sharif Khan-Bennett[1]*
[1]School of Physics and Astronomy, University of Birmingham, Edgbaston, Birmingham, B15 2TT, UK

27 March 2021

**ABSTRACT**
Upcoming surveys from new-generation radio observatories such as the Square Kilometer Array (SKA) will generate an unprecedented volume of astronomical data. Object classification is an essential aspect of investigations, however, it will soon be unfeasible using current classification techniques; automated classification will become essential. This investigation proposes the development of a Convolutional Neural Network (CNN) to identify features in the Galactic Centre (GC) which may have played a role in the formation of Non-Thermal Filaments (NTFs). The classification tools developed in investigations like this will become useful in the future when investigating dimmer NTFs in the GC as well as NTFs found in external galaxies. Additionally, understanding the formation of NTFs will reveal a wide range of new physics relating to galactic nuclei.

## 1 INTRODUCTION

The development of SKA Pathfinder telescopes indicates the beginning of a new-generation of Radio surveys. New surveys will be able to detect much dimmer objects as well as being able to cover much larger areas of the sky, see figure 1. As a result, the volume of data needing to be processed becomes huge and the use of source detection tools such as Agean Hancock et al. (2012, 2018) and FilFinder Koch & Rosolowsky (2015) become inappropriate due to the amount of user interaction required. This project sets out to develop a CNN to identify NTFs and other sources in the GC. NTFs are often used to study the magnetic field in the GC, however the mechanism causing their formation is currently unknown. Several models have been put forward and many of them require the presence of another object to initiate its formation. The CNNs will be used to search for these objects in the vicinity surrounding each NTF in the hope of lending weight to one of the models.

Section 2.1 outlines some of the theory of NTFs including some proposed formation models, section 2.2 discusses machine learning (ML) techniques, section 3 goes into more detail on how the NTFs will be studied in conjunction with external sources and section 4 outlines the expected timeline of the project.

## 2 THEORY

### 2.1 Non-Thermal Filaments

Filaments are highly polarised synchrotron emission sources Paré et al. (2019). They are extremely long and thin; $10-40pc$ long and $\leq 0.5pc$ wide Morris (2007). The NTFs are formed of highly relativistic electrons spiralling along magnetic field lines Yusef-Zadeh et al. (1984). The majority of the NTFs are approximately perpendicular to the galactic plane indicating a bipolar magnetic field in the region; the current consensus supports a pervasive poloidal magnetic field extending across the central $200-300pc$ of the galaxy Morris (2007). Due to their largely monotonic curvature within the highly turbulent interstellar medium (ISM) (see figure 2) an implied rigidity requires the magnetic field strength to be $10\mu G - 1mG$ Morris (2007), see figure 2.

Despite what is currently known about NTFs concerning the surrounding magnetic field, there is currently no agreed-upon model explaining how they were formed, in particular, what the source of the relativistic electrons are and what causes their acceleration. Some of the proposed sources include molecular or ionized gas clouds, supernova remnants (SNRs) or pulsar wind nebulae (PWNe) Shore & LaRosa (1999); Barkov & Lyutikov (2019); Bicknell & Li (2001). Due to the similarities between NTFs and their uniqueness to the GC, these NTFs all probably arise from a common formation mechanism Gray et al. (1995). It should therefore be expected that the source of the electrons would be present in all cases of NTFs and with a similar relative orientation. Multiwavelength data can be used in conjunction with image classification algorithms to identify the sources in the vicinity of each filament. Trends in the frequency of each of the candidates may lend weight to some of the models.

The proposed formation theories fall into several classes according to Bicknell & Li (2001) as outlined below:

(i) Interaction between a star or cluster of stars with the ISM.
(ii) Interaction between the galactic wind and molecular clouds.
(iii) Electrodynamic models (including MHD waves.)
(iv) Shock Waves in the ISM.
(v) Morphologically unusual SNRs
(vi) Exotic models including the presence of cosmic strings.

#### 2.1.1 *Star Trails*

A model proposed by Gray et al. (1995); Nicholls & Strange (1995) suggests that the NTFs could be caused by the supersonic passage of a star through the ISM causing a massive stellar wind. A subsequent nearby supernova could then inject the trail with energetic particles, causing its illumination. This model was used to explain the source of the kinks in the NTF "The Snake," whereby gravitational interactions alter the path of the supersonic star, resulting in sudden bends. This model has been somewhat disregarded however due to the NTFs

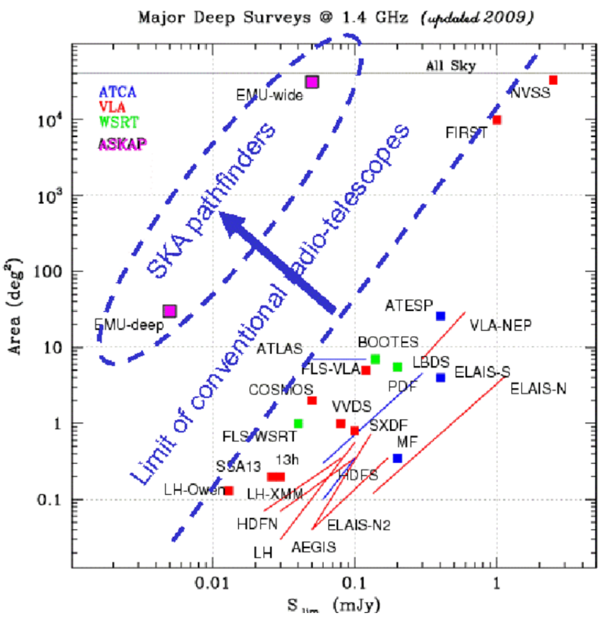


**Figure 1.** Future SKA surveys in comparison to current surveys. The most sensitive surveys are in the bottom left, where the top right are surveys which cover the widest area of the sky. The dashed line shows the limit of conventional radio surveys. It is clear from this image that SKA Pathfinders such as the Australian SKA Pathfinder (ASKAP) will generate huge amounts of data previously unavailable to us. Image courtesy of Norris (2011); Prandoni & Seymour (2015)

exhibiting curves which are not consistent with the expected orbital trajectories in the region.

### 2.1.2 *Molecular Clouds and Plasma Tails*

Shore & LaRosa (1999) proposed a model based off an analogy with cometary plasma tails. Here, the galactic wind is suggested to have encountered a molecular cloud causing it to be enveloped by a magnetic field and resulting in a current sheet forming in the cloud's wake. This field is then amplified by the stretching of the wake by the ram pressure of the galactic wind. Acceleration of the electrons is caused by turbulence in the wake. This theory may carry weight as molecular clouds have been detected in the vicinity of the radio Arc Yusef-Zadeh et al. (1984), on the other hand, these clouds are absent from the "Snake" Bicknell & Li (2001). Additionally, the detection of NTFs lying parallel to the galactic plane by Lang et al. (1999); LaRosa et al. (2001) appear to contradict this theory.

### 2.1.3 *Magnetohydrodynamic (MHD) waves*

Proposed by Sofue (2020), it is suggested that MHD waves are ejected from Sgr A* or by multiple supernovae and are funnelled by the magnetic field resulting in thread-like structures being viewed when observed tangentially.

### 2.1.4 *Shock Fronts*

One of the original proposals by Yusef-Zadeh et al. (1984) suggested that the linear NTFs could be the edge of a two-dimensional shock front which appears limb-brightened as a result of viewing angle. Some of the stated problems with this model suggest that the inhomogeneities in the GC would have caused many more irregularities and breaks in the NTFs than what is observed.

### 2.1.5 *Jet Streams from pulsar wind nebulae (PWNe) reconnecting to the ISM*

Barkov & Lyutikov (2019) suggested that NTFs are a result of streams of relativistic particles escaping from PWNe and travelling along magnetic flux tubes which have become stretched radially by the galactic wind to reach the ISM. In addition to PWNe, SNRs are suggested as a potential source for the relativistic particles.

## 2.2 Image Classification

### 2.2.1 *Convolutional Neural Networks*

Neural Networks (NN) are a type of deep learning algorithm. They are inspired by biological neurons in terms of how they are connected in layers to analyse input data Fukushima (1980). Data is sent forwards through the network where the neurons in each layer become sensitive to certain features in the data. Layer by layer, more complex features can be identified with the final layer producing a prediction of what the data represents. A defined loss function then provides a measure of the performance by comparing the output of the NN to the labels provided in the "training data." Then, backpropagation occurs where the sensitivity (or weight) of each neuron is adjusted in a process called "stochastic gradient descent". This attempts to converge upon a set of parameters (weights and biases) for all neurons which produce the smallest loss. This is done iteratively over large amounts of data in the training set such that the NN learns aspects from a wide range of data. Consequently, the data used to train the NN must be fully representative of the unseen data such that the NN can be generalised Abadi et al. (2015).

The output of a single neuron, $y$, in the network is given by:

$$y = f\left(\sum_{j=1}^{n} w_j x_j + b_j\right) \tag{1}$$

where $n$ is the number of connected neurons from the previous layer, $x_j$, $w_j$ and $b_j$ is the input, weight and bias from the $j^{th}$ neuron in the previous layer and $f$ represents the "activation function" which provides the non-linearity required to model complex data. Common activation functions include $ReLu$, $sigmoid$ and $tanh$. This project will most likely use $ReLu$ as it has been proven to outperform the other activation functions in terms of speed and reliability Changpinyo et al. (2017). It is given by $f(x) = max(x, 0)$

In one epoch, a batch of data is sent forwards through the layers, the loss is calculated and backpropagation takes place such that the following epoch produces a smaller loss. The learning rate is defined as the size of the step taken when altering the weights and biases towards the global minima during gradient descent. This has to be chosen with care and with respect to the problem at hand; too small of a step will result in the optimiser getting stuck in local minima, whereas too large of a step will result in the optimiser struggling to converge Abadi et al. (2015).

CNNs are commonly used to analyse visual data as they retain the 2D spacial information about the image. Here, layers apply filters to the data which train to learn different features in the image.

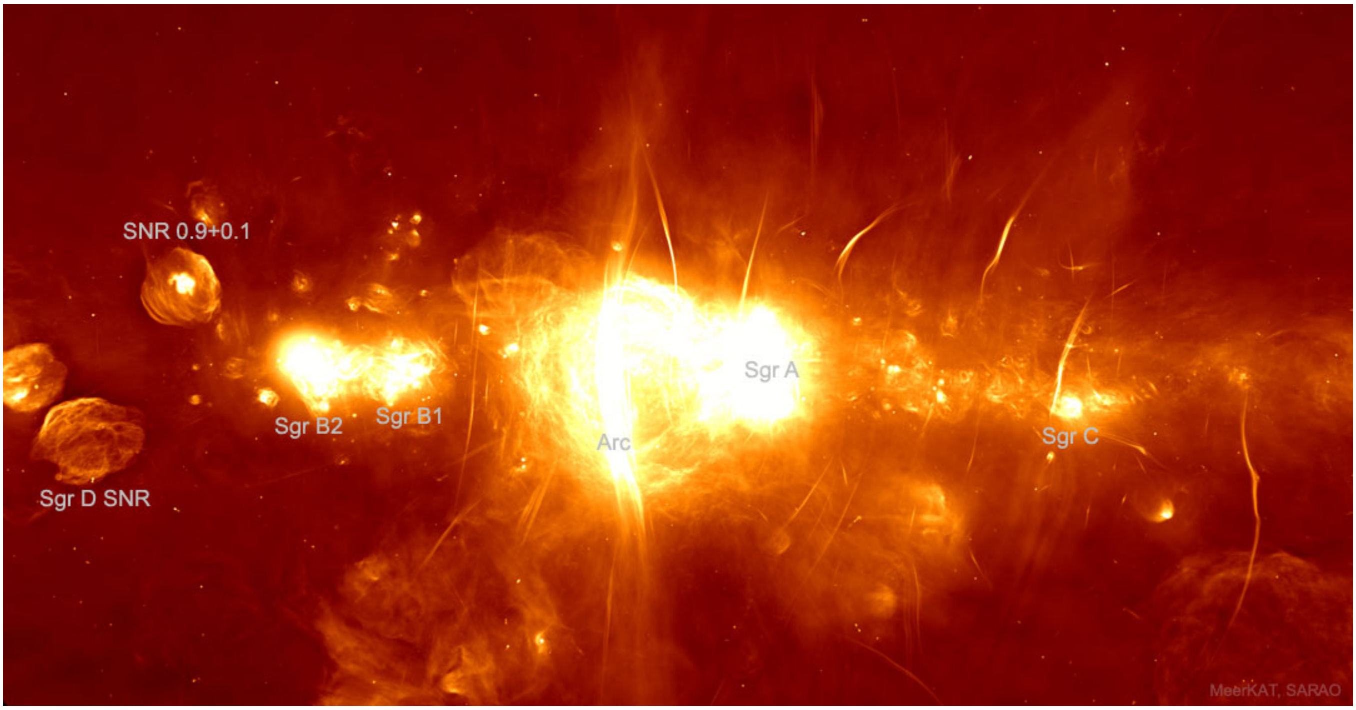


**Figure 2.** The inaugural image of the MeerKAT array of the Galactic Centre, Sagittarius A*. The image features many NTFs, the bright thread-like structures predominantly seen above the galactic plane. The "Arc" has been labelled and has been one of the focuses of research into the filamentary structure in the GC, it is a dense region of many aligned NTFs. Image courtesy of SARAO (SARAO)

Additionally, pooling layers are used which set a square region of pixels to a single value, either the mean or max value Alhassan et al. (2018). This removes small details in the images to avoid overfitting (see section 2.2.2) thus also improving computation time. See figure 3 for an example of a typical CNN architecture.

### 2.2.2 *Regularization*

One of the main problems with this process will be the risk of overfitting. This is when the model starts to fit to all the random noise unique to a training set. It results in poor generalisation to unseen data and is characterised by the loss curve generated for the test set diverging from that of the training set. This problem can be combated by the use of regularization techniques. One common technique is called "dropout" whereby a proportion of neurons are randomly selected to have their outputs set to zero. This results in the model having to create a range of channels for features in the data meaning that it will create more robust connections and generalise better, rather than just "memorising" the training set Abadi et al. (2015).

Early stopping is another technique that will be used to try and avoid overfitting. This is when the loss curves for the training set and test set are monitored in real-time. The training can then be stopped once the test loss curve begins to diverge from that of the training set.

### 2.2.3 *Image Processing*

As mentioned above, machine learning techniques require a vast amount of training data for the algorithm to perform with high accuracy. Since there are a limited number of images of the sources mentioned in section 2.1 to train with, creative solutions will need to be employed to increase the size of the training set.

Image augmentation will be used to increase the size of the training data. Here, rotations and inversions can be applied to the images. This will not affect the science because the observation of NTFs and the surrounding environment is not affected by their orientation with respect to the observer.

Another technique that will be employed is the use of a deep convolutional general adversarial network (DCGAN). This will involve the creation of a "generator" and a "discriminator" which both have the same architecture as the CNN described in section 2.2.1. The role of the generator is to create realistic data from random noise, while the role of the discriminator is to be able to tell the difference between real and fake data. Over many iterations, the generator gets better at creating fake data and the discriminator gets better at identifying the fakes. The system reaches equilibrium when the discriminator can no longer identify the real data from the fake data Abadi et al. (2015).

The data gained from the application of the image augmentation technique will be fed into the discriminator in the DCGAN to produce even more available data which, along with the augmented and original images will make up the training set for the CNN.

## 3 METHODS

Each of the theories in section 2.1 rely on the presence of some other source. Independent detection of one of these sources either by direct imaging or by inference from a secondary effect will add weight to the relevant theory. This can be done by defining a search area around each filament and using a CNN to search through all the data in the hope of identifying all instances of the proposed sources.

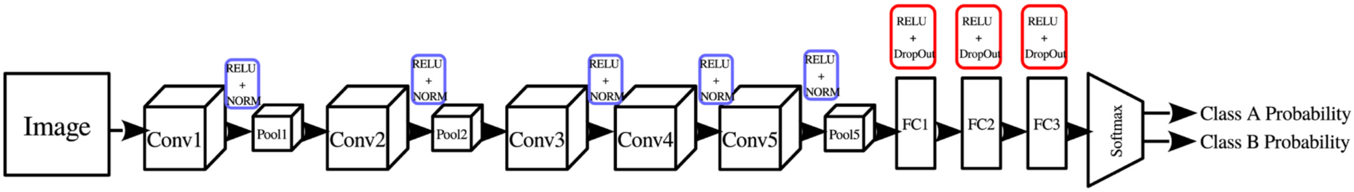


**Figure 3.** Example of the architecture of a CNN. This network has 5 convolutional layers separated by 5 pooling layers. At the end, there are then three fully connected (dense) layers which include a dropout function. The final layer is a "softmax layer" which normalises the output of the previous layer to represent a probability distribution over all the possible outputs. Image courtesy of Aniyan & Thorat (2017)

Each instance can then be validated in terms of having the correct orientation to the NTF. Then, by applying statistical analysis the above theories can be ranked in likelihood based on the results from this investigation.

There are already many tools which have been developed to find sources and filaments in radio images, some include the previously mentioned FilFinder Koch & Rosolowsky (2015) and Agean Hancock et al. (2012, 2018). FilFinder can be used on the data from the GC to find the locations and orientations of filaments with respect to the galactic plane. Alternatively, results could also be quoted from literature. Agean and similar tools can be used to search the area surrounding the filaments and multiwavelength analysis may also be required to more accurately identify some of the sources such as stellar clusters and SNRs which are more prominent in other wavebands.

The results from these "non ML techniques" can be used to generate labelled datasets and to ensure that the CNN is correctly identifying sources. The aim is to produce a CNN which can identify filaments and other sources in a much shorter timeframe and with little or no drop in accuracy. Image augmentation and GANs will be used to ensure a large enough training set is available. The machine learning techniques will be developed using TensorFlow through the Keras API.

In addition to analysing current data, this investigation sets out to lay down some of the framework and techniques which could be used once dimmer sources in the GC and sources in external galaxies are detected by next-generation telescopes such as the SKA.

## 4 TIMELINE

This project will take place over the unusual COVID-19 period and at the time of writing it is unknown whether the UK or Birmingham will re-enter lockdown which could disrupt this investigation. Thankfully, the majority of the work can be done on personal laptops as we have been granted local access to University of Birmingham's BlueBEAR HPC service which will prove to be useful when running some of the computationally intensive programs. Figure **??** outlines a proposed timeline for the project.

## REFERENCES


Abadi M., et al., 2015, TensorFlow: Large-Scale Machine Learning on Heterogeneous Systems, `https://www.tensorflow.org/`

Alhassan W., Taylor A. R., Vaccari M., 2018, MNRAS, 480, 2085

Aniyan A. K., Thorat K., 2017, ApJS, 230, 20

Barkov M. V., Lyutikov M., 2019, MNRAS, 489, L28

Bicknell G. V., Li J., 2001, Publ. Astron. Soc. Australia, 18, 431

Changpinyo S., Sandler M., Zhmoginov A., 2017, CoRR, abs/1702.06257

Fukushima K., 1980, Biological Cybernetics, 36, 193

Gray A. D., Nicholls J., Ekers R. D., Cram L. E., 1995, ApJ, 448, 164

Hancock P. J., Murphy T., Gaensler B. M., Hopkins A., Curran J. R., 2012, MNRAS, 422, 1812

Hancock P. J., Trott C. M., Hurley-Walker N., 2018, Publ. Astron. Soc. Australia, 35, e011

Koch E. W., Rosolowsky E. W., 2015, MNRAS, 452, 3435

LaRosa T. N., Lazio T. J. W., Kassim N. E., 2001, The Astrophysical Journal, 563, 163

Lang C. C., Anantharamaiah K. R., Kassim N. E., Lazio T. J. W., 1999, ApJ, 521, L41

Morris M., 2007, arXiv e-prints, pp astro–ph/0701050

Nicholls J., Strange E. L., 1995, The Astrophysical Journal, 443, 638

Norris R., 2011. pp 21 – 24, doi:10.1109/eScienceW.2010.13

Paré D. M., Lang C. C., Morris M. R., Moore H., Mao S. A., 2019, ApJ, 884, 170

Prandoni I., Seymour N., 2015, Revealing the Physics and Evolution of Galaxies and Galaxy Clusters with SKA Continuum Surveys (`arXiv:1412.6512`)

SARAO, APOD: 2019 July 8 - The Galactic Center in Radio from MeerKAT, `https://apod.nasa.gov/apod/ap190708.html`

Shore S. N., LaRosa T. N., 1999, ApJ, 521, 587

Sofue Y., 2020, PASJ, 72, L4

Yusef-Zadeh F., Morris M., Chance D., 1984, Nature, 310, 557